

## Diamond and Cubic Boron Nitride: Properties, Growth and Applications

Peer-reviewed author version

Soltani, A.; Talbi, A.; MORTET, Vincent; BenMoussa, A.; Zhang, W. J.; Gerbedoen, J-C; De Jaeger, J-C; Gokarna, A.; HAENEN, Ken & WAGNER, Patrick (2010)  
Diamond and Cubic Boron Nitride: Properties, Growth and Applications. In: Ferro, G.; Siffert, P. (Ed.). 2010 WIDE BANDGAP CUBIC SEMICONDUCTORS: FROM GROWTH TO DEVICES, p. 191-196.

Handle: <http://hdl.handle.net/1942/16978>

# Diamond and Cubic Boron Nitride: Properties, Growth and Applications

A. Soltani<sup>a</sup>, A. Talbi<sup>a</sup>, V. Mortet<sup>b,c</sup>, A. BenMoussa<sup>d</sup>, W.J. Zhang<sup>e</sup>, J-C Gerbedoen<sup>a</sup>, J-C De Jaeger<sup>a</sup>, P. Pobedinskas<sup>b,c</sup> and A. Gokarna<sup>a</sup>, J-F Hochedez<sup>d</sup> and K. Haenen<sup>b,c</sup>

<sup>a</sup>*Institut d'Electronique, de Microélectronique et de Nanotechnologie, F-59652 Villeneuve d'Ascq, France.*

<sup>b</sup>*Institute for Materials Research, Wetenschapspark 1, B-3590 Diepenbeek, Belgium, Division IMOMEC.*

<sup>c</sup>*IMECvzw, Wetenschapspark 1, B-3590 Diepenbeek, Belgium.*

<sup>d</sup>*Royal Observatory of Belgium, Circular Avenue 3, B-1180 Brussels, Belgium.*

<sup>e</sup>*Center of Super-Diamond and Advanced Films, City University of Hong Kong, Hong Kong SAR, China.*

**Abstract.** Since their first synthesis, cubic boron nitride (c-BN) and diamond thin films have triggered a vivid interest in these wide band gap materials for many different applications. Because of superior properties, c-BN and diamond can be applied in optic, electronic and acoustic for high performances devices. In this discussion, we first describe briefly the properties of c-BN and diamond and we review both the growth techniques and the progresses achieved in the synthesis of c-BN and diamond, in the second part, characteristics of new c-BN and diamond UV detectors for solar observation are reported. These photo-detectors present extremely low dark current, high breakdown voltage, high responsivity and stability under UV irradiation. Finally, diamond based acoustic devices and sensors are presented. High frequency acoustic wave devices can be design for high frequency filtering or sensing applications. Diamond/AlN micro-cantilevers are excellent platform for sensor applications.

**Keywords:** diamond, cBN, AlN, sputtering, CVD, doping, photodetector, RF resonator, actuator, sensor.

**PACS:** 81.05.-t, 81.15.-z, 81.16.-c, 81.20.-n, 81.20.-n, 85.30.-z, 85.50.-n, 85.60.-q, 85.85.-j

## 1. INTRODUCTION

The compounds of the B/C/N system as cubic boron nitride (c-BN) and diamond possess exceptional properties. Modern key technologies as microelectronics, power devices, optoelectronics or micro-and-nano-systems lie in mastering of these new materials production.

Whereas natural diamond occurs, only synthetic cubic boron nitride (c-BN) can be growth. In analogy to carbon, boron nitride can be synthesized in two major crystalline polytypes, the hexagonal (h-BN) and the zinc-blende structure (c-BN), related respectively to the  $sp^2$  and the  $sp^3$  hybridation of the chemical bonding of both atomic species, with similar physical properties to graphite and diamond. Boron nitride is isoelectronic to graphitic carbon and cBN and diamond are both metastable. The carbon-carbon bond is purely covalent whereas the boron-nitrogen bond is partially ionic. These very light materials have unique properties including high degree of hardness (cBN is the second strongest and hardest material after diamond), strength, wear resistance and robust to radiation. Unlike diamond, c-BN is chemical inertness readily with ferrous metals, cobalt and nickel (or with an oxide) and has a high resistance to oxidation in air up to high temperature (1200°C) making it even more attractive for tooling applications. Furthermore, these semiconductors are suitable for a broad range of electronic applications. Indeed, cBN has the widest energy band gap of all III-V compound semiconductors (~6.4eV compared to 5.5eV for diamond) and it is transparent over a large spectral range<sup>1</sup>. Since cBN can be easily doped both p- and n-type, it is more attractive than diamond<sup>2</sup>. cBN has the highest thermal conductivity just after diamond (13Wcm<sup>-1</sup>K<sup>-1</sup> for cBN - 24Wcm<sup>-1</sup>K<sup>-1</sup> for diamond at 300K) and both undoped material have a high electrical resistivity. These properties make these materials excellent candidates for application in power electronics, micro-nano-mechanical resonator, actuator or sensor.

## 2. CUBIC BORON NITRIDE GROWTH

The synthesis of cBN can be performed in various ways, usually at high temperature ( $T \geq 1000K$ ) and high pressure ( $P > 4GPa$ ), involving a change from the hexagonal to cubic phase<sup>3</sup>, or at low temperature and high pressure, the rhombohedral phase turns into cBN.

C-BN can be obtained by both Chemical Vapor Deposition (CVD), Physical Vapor Deposition (PVD) or pure ion beam deposition. It has been shown by many authors that the growth process requires intense

bombardment with energetic particles [ $200(\text{eV}\cdot\text{amu})^{1/2}$  to  $1(\text{keV}\cdot\text{amu})^{1/2}$ ] <sup>4,5</sup>. The threshold value for the formation of high cBN content is variable and depends on the deposition technique. This is due to not well defined energy bombarding ions involving a more or less wide distribution of energies. This method allows to reduce the concurrent formation of the stable hexagonal soft h-BN. In most cases, cBN films normally grow via amorphous (aBN) and turbostratic (tBN) interfacial layers, which are soft and moisture-sensitive, on a foreign substrate (such as silicon) <sup>6</sup>. The interfacial tBN layer acts as an incubation medium for cBN nucleation. Whatever the method used (PVD or CVD), the layer inevitably withstands with significant build-up of compressive stress (5-20GPa) after deposition and delamination or cracking of the film can occur. So, this problem limit the practically achievable thickness of c-BN coatings larger than 200nm <sup>7</sup>.

Another disadvantage of these deposition methods is the low growth rates and the layer is made of nano-crystallites with grain boundaries which are harmful to opto- and micro-electronics applications. Therefore, the substrate, its surface pretreatment and its temperature are key criteria for adhesion and quality of deposited cBN films <sup>8</sup>. Furthermore, to obtain high purity cBN films, it is necessary to be close to stoichiometry and to get residual oxygen level below 4% <sup>9</sup>.

To improve adherence and to reduce the stress of film during growth, different solutions have been tested: (i) stacks of a metal buffer multilayer (W, WC, TiAlN, TiN, Ti(B,C)...) followed by a thick layer such as B<sub>4</sub>C or BCN and a cBN film; (ii) hBN/cBN multilayers stacks...

Finally, to improve the adherence and reduce the stress, a two steps process has been used based on a post-treatment or an in-situ hard process to nucleate high cBN sites density followed by a specific soft process permitting the growth of a thick, low stress and high quality cBN film. By this method, high growth rate ( $>0.2\mu\text{m/h}$ ) is obtained. By this way, an epitaxial growth of c-BN films can be successfully realized using fluorine-assisted growth and introducing a diamond interlayer <sup>10</sup>. Analog to diamond growth, fluorine will etch especially graphitic phase.

In this work, high quality, thick and adherent cBN films have been grown at high temperature ( $\sim 900^\circ\text{C}$ ). The films were deposited on diamond-coated silicon substrates in an electron-cyclotron-resonance microwave plasma (ECR-MW) CVD system using a He-Ar-N<sub>2</sub>-BF<sub>3</sub>-H<sub>2</sub> gas. The introduction of fluorine chemistry into the plasma reduced the film stress and enabled the growth of thick ( $>2\mu\text{m}$ ) cBN films with relatively large crystallites. Diamond films using as substrates for cBN growth were deposited on silicon (001) wafers with a routine microwave plasma CVD method <sup>10</sup>.

The films present a columnar growth of cBN with an epitaxial growth at the interface with diamond crystallites. The film stress is low (2GPa), contributing to the superior adhesion and stability in a humid environment. The hardness and the elastic modulus of films obtained are quite high (75GPa and 800GPa, respectively).

### 3. DIAMOND GROWTH

Artificial growth of diamond has been developed in the second part of the 20<sup>th</sup> century. First artificial diamonds were produced by HPHT, latter it was shown that diamond can be grown at low pressure by CVD process. Since then CVD diamond growth techniques were developed and optimized.

It is reckoned in the field that atomic hydrogen has a significant role in low pressure growth of diamond. Several methods of hydrogen activations exist, the thermal activation by hot filament and the electrical activation by microwave plasma. These two methods are comparable in general and in terms of gas compositions, pressure and substrate temperature. However, the substrate size is limited in MWPECVD in contrary to hot filament, but the grow rate can be significantly higher. Nonetheless, large area deposition of Nano-Crystalline Diamond (NCD) by MW-PECVD using surface waves have been reported recently <sup>11</sup>. One of the main issues in diamond growth on a foreign substrate is diamond nucleation. Even if the nucleation mechanism is still not well understood, two methods have been proven to be efficient: mechanical seeding and bias enhanced nucleation <sup>12</sup>. With the use of the recently developed detonation nanodiamond colloid, it has been proven that nanodiamond seeds can be efficiently dispersed on samples' surfaces before growth <sup>13</sup>. This technique leads to the highest nucleation densities achievable but one can also observed a lower adherence of thick diamond films compared to films deposited on substrates nucleated with others methods. Deposition conditions of diamond by CVD techniques have been widely studied and several diamond film crystallinities have been obtained: (ultra-)nanocrystalline diamond, microcrystalline diamond, highly oriented diamond, hetero- and homo-epitaxial films. With extremely high re-nucleation rate, films grown either in argon rich / hydrogen poor plasmas or with bias results in ultra-nanocrystalline diamond films with grains sizes below 10nm. Other nanocrystalline films are grown in hydrogen rich plasma as microcrystalline films; they consist in general of thin films (bellow  $1\mu\text{m}$ ) with columnar structure. High nucleation density is a key point for the growth of this material <sup>14</sup>. Thick microcrystalline or polycrystalline diamond films have in general a (110) texture. The texture varies with the process parameters including impurities as nitrogen that promote (100) texture. By a careful control of the nucleation and the texture, highly oriented and heteroepitaxial diamond films have been obtained.

So far, best results of heteroepitaxial diamond growth have been obtained on Iridium, one inch in diameter heteroepitaxial films has been recently reported and are commercially available<sup>15</sup>. Epitaxial growth has been extensively studied for substrate size enlargement and for electronic applications. Diamond has been a promising material for high frequency and high power electronics despites several severe drawbacks: small size of substrate, limited number donor and acceptor impurities, high activation energy, incorporation, and complex processing...

Nitrogen, phosphorous (P) and boron (B) are the only reckoned electrically active impurities of diamond nowadays. All have high activation energy, meaning that at room temperature, only a minute amount of impurities are ionized. Activation energy of nitrogen is so high that it does not have practical applications. Successful incorporation of P or B with good electric properties has been only achieved by PECVD. The qualities of the films are strongly dependent on the substrate orientation. Best p-type diamond films were obtained on (100) substrates<sup>16</sup> while the best n-type layers were obtained on (111) substrates<sup>17</sup>. This problem limits the fabrication of good bipolar diamond devices. The recent demonstration of P incorporation on (110) oriented diamond might be a solution to this problem.

**TABLE 1:** Other properties of wide band gap materials for our applications.

Physical properties @ 300K	wAlN	cBN	diamond
Band gap (eV)	6.1 (direct)	6.4 (indirect)	5.5 (indirect)
Mass density (g.cm <sup>-3</sup> )	3.25	3.45	3.52
Breakdown voltage (×10 <sup>6</sup> V/cm)	~ 1.5	2-6	10
Resistivity (Ω.cm)	>10 <sup>15</sup>	>10 <sup>15</sup>	>10 <sup>16</sup>
Dielectric constant	8.5	7.1	5.7
Electron (hole) mobility (cm <sup>2</sup> /V.s)	300 (14)	200 (500)	2200 (1600)
Ionization Energy to create e-h pair (eV/ehp)	18.8	17.6	13
Coefficient de dilatation thermique (×10 <sup>-6</sup> °C <sup>-1</sup> @ 400°C)	4.1-5.2	4,8	0,8
Vitesse acoustique (km.s <sup>-1</sup> )	6.3-10.1	~ 9.6-17.4	~ 11-18
Dureté (kg.mm <sup>-2</sup> )	800	4000-5000	9000
Module de Young (GPa)	308	820	1140

## 4. APPLICATIONS

Since their first synthesis, exceptional properties of c-BN, AlN, and diamond (Table 1) have arisen the interest in these materials for many different applications. Firstly, they have been used for mechanical applications since C-BN and diamond are the two hardest known materials. Both c-BN and diamond have high thermal conductivity and they are transparent in a wide range of the electromagnetic spectrum that allows their use in optical windows and thermal management. These wide band gap materials have been also forseen to be used in semiconductor devices operating in harsh environments as solar blind UV detectors in space (LYRA project). These materials possess desirable properties for MEMS applications as microcantilevers<sup>18</sup> and electro-mecanical devices as SAW devices operating at high frequencies<sup>19</sup>. In addition, the biocompatibility of diamond makes it suitable for biosensors applications.

### 4.1 X-UV Photodetectors

The goal of this work is to develop large single-pixel detectors (>3mm diameter) dedicated for the fabrication of imaging arrays of micro-pixel structures for space applications<sup>20</sup>.

Knowing the harsh space environment, radiation-hardness of Wide Band Gap Materials (WBGm) could significantly extend the performance and the lifetime of the sensor. As defined for applications in space, solar-blind photodetector requires a detector cut-off wavelength below 150nm wavelength which is insensitivity to the solar continuum spectrum or photons of lower energy<sup>21</sup>.

Another important gain is the mobility of charge carriers in WBGm which can be very high (Table 1). It enables a very fast response of detectors opening capabilities for higher cadence observations and new photon-counting readout schemes.

However, under VUV the penetration depth  $1/\alpha(\lambda)$  drops drastically to few nanometers as for the Lyman-alpha line (121.6nm). In the technological process, the surface treatment is a significant step to obtain low surface recombination velocities and consequently an improvement of the sensor sensitivity. Furthermore, it is crucial to optimize the photo-electrons collection close to the surface by means of a planar configuration of the electrodes<sup>22</sup>.

Different types of semiconductor detectors have been developed (in order of increasing manufacturing complexity): Metal-Semiconductor-Metal (MSM) diodes, MSM photoconductors and PIN photodiodes. These

carriers created by photoelectric effect are separated by the electric field due to either the built-in potential (MSM diode or PIN) or the applied voltage (MSM photoconductor), produce a current proportional to the photon flux.

The choice of the photosensitive diode depends on their inherent properties and various constraints, not only related to performance but also to the fabrication process: the photoconductors and Schottky-diodes can be built with co-planar structures, making their production easier than PIN diodes consisting of different doped layers and that requires an etching step.

Usually, photoconductive devices have a high sensitivity and may benefit from internal photoelectric gain (in constant voltage operating mode). Since they need a bias, they have low impedance but usually a higher dark current than Schottky- or PIN- diodes. The latter provides the advantages of bias-free operation, very low background dark current and fast response.

For MSM photodetectors, various criteria require consideration when designing a UV photodetector for space applications: (i) the optical wavelength of interest (10 to 200nm), (ii) the thickness of semiconductor thin film, (iii) material nature and structure and (iv) the design and the metallic electrodes content.

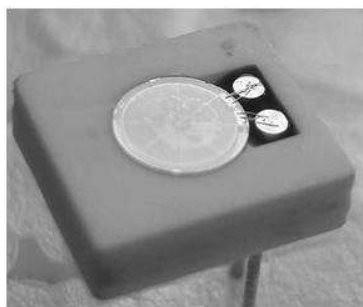
MSM photoconductor consists of a semiconductor sample with two ohmic contacts where a potential difference is applied between them while the MSM photodiode is essentially two Schottky barrier diodes back-to-back fully depleted under sufficient bias. MSM photoconductors are different to MSM photodiodes in several important ways: current is carried both by minority and majority carriers in the photoconductor, and the gain can be higher than unity depending primarily on the ratio of the minority carrier lifetime to the majority carrier transit time.

Figure 1 show the solar spectral irradiance measured in space. It can be noted that the visible solar continuum (from 400-to 700nm) is 4 to 5 orders of magnitude brighter than the VUV part of the spectrum (from 10nm to 122nm). A good rejection of the wavelength above 150nm (e.g. more than 4 orders of magnitude) constitute the ideal sensor for VUV solar observations. The quantum efficiency of a diamond MSM photoconductor, wAlN MSM and cBN photodiodes are also shown in Figure 1. These materials present a large band gap and therefore its fluctuations which act as a noise, are much reduced, permitting room temperature operations. The performances obtained on MSM photodetectors are given in Table 2.

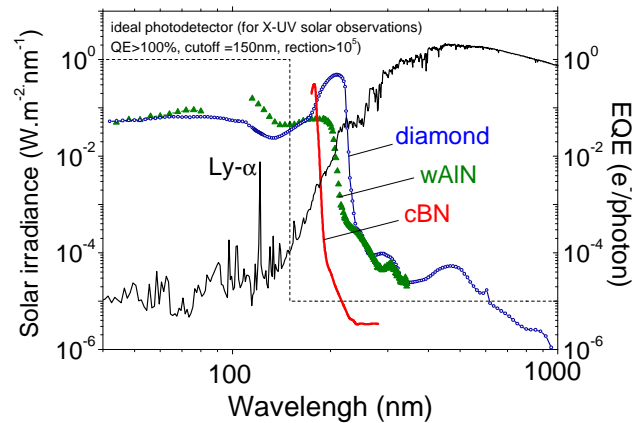
**TABLE 2.** Summary of performances obtained on MSM photodetectors.

	Dark current	Responsivity (mA/W)	Cut-off $\lambda_c$ (nm)	Rejection rate
cC	1pA (+5V)	48 (@ 210nm)	225 (5.5 eV)	$1.35 \times 10^2$ (210/400)nm
wAlN	100 fA (+100V)	2 (@ 200nm)	203 (6.1 eV)	$10^3$ (200/360)nm
cBN	9.3pA (+50V)	32 (@ 180nm)	193 (6.4 eV)	$1.05 \times 10^2$ (180/250)nm

The active area sensor has an inner diameter of 1 to 5mm. The interdigitated separation varies from 1  $\mu\text{m}$  to 10  $\mu\text{m}$  and the metal fingers width varies from 2 to 5  $\mu\text{m}$ . The details on the technological process are given in [22, 23]. An optimized circular geometry of interdigitated electrodes permits to improve response uniformity, high efficiency of charge detection and very low dark current at room temperature<sup>23</sup>.



(a)



(b)

**FIGURE 1:** (a) Photo of diamond MSM photoconductor; (b) The solar spectral irradiance measured in space and from Earth (left ordinate axis) compared with the quantum efficiency (right ordinate axis) of an ideal and experimental wide band gap detectors for solar observations (diamond, wAlN and cBN MSM).

## 4.2 Diamond capabilities for RF mechanical resonators

One of the most attractive applications of diamond is the High Velocity Surface Acoustic Wave devices (HVSAS). A great progress in research and development has been carried out to make CVD diamond film

compatible to these devices. Several kinds structures based on poly-crystalline or nanocrystalline diamond coupled to a piezoelectric thin film such as ZnO, AlN or LiNbO<sub>3</sub> have been investigated. It has been found that HVSAW device can be achieved by such structures when diamond thickness is chosen higher than wavelength two times. One of the most promising multilayer structures is AlN/Polycrystalline diamond (Poly-diamond) providing SAW velocities in excess of 11km/s and electromechanical coupling coefficient ( $K^2$ ) up to 2%<sup>24</sup>. To achieve high  $K^2$  in the HVSAW device, a high value of AlN normalized films thickness ( $kh=2\pi \times h/\lambda$  where  $h$  is the AlN film thickness and  $k$  is the wavelength) is needed. From this point of view, the fabrication of this kind of acoustic wave device is not in perfect agreement with conventional silicon technologies. Since few last years, a particular attention was done on the new design of micro-electromechanical (MEMS) resonators technologies based on piezoelectric transduction. Among these design, AlN Contour-Mode MEMS resonator (CMR)<sup>25</sup> and thin film plate acoustic wave resonators (FPAR)<sup>26</sup> are particularly promising. These new designs of acoustic wave devices permit to increase drastically the operating frequency and the quality factor by more than one or two magnitude compared to conventional HVSAW devices for the same mechanical wavelength. Until now, operating devices based on this technology giving high performance have been achieved on AlN or ZnO thin films for devices applications dedicated to frequency reference and integrated circuits. However, robustness of these devices is limited when it works in harsh environments and when it must withstand high power up to few Watts. Therefore, integration of piezoelectric material on diamond thin films permits to obtain mechanical resonators with high performance for wireless communications thanks to its thermal and mechanical properties. Theoretical analyses have been performed in order to evaluate the capability of AlN/diamond structure as FPAR resonator. Figure 2 shows the dependence of the elastic wave velocity and  $K^2$  for the lowest symmetric Lamb wave mode ( $S_0$ ) as a function of AlN  $kh$  for both AlN and AlN/diamond devices. We can note clearly that  $S_0$  mode properties are better on the AlN/diamond structure compared to the AlN one. Furthermore, it offers at the same time, high elastic wave velocity (more than 10km/s) and high  $K^2$  (more than 3%) in large  $kh$  range (1 to 4).

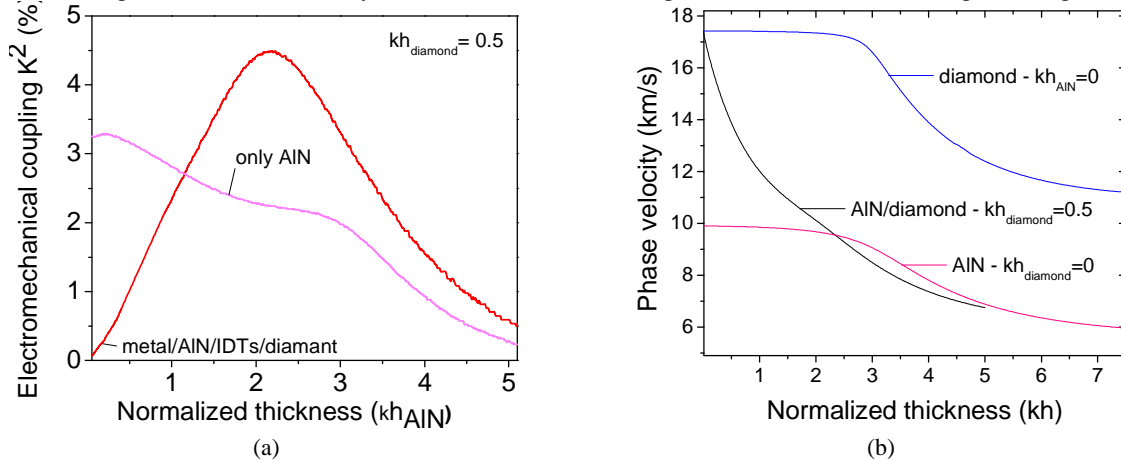


FIGURE 2. (a) AlN and AlN/diamond  $K^2$  corresponding to FPAR mode versus AlN normalized thickness, (b) AlN, diamond and AlN/diamond phase velocity corresponding to FPAR mode versus normalized thickness.

### 4.3 NCD thin film with piezoelectric material for high-frequency mechanical actuator

Diamond thin film based resonant structures offer several advantages over silicon and other thin-film materials used in micro- and nano- fabrication. As resonant structure, nano-crystalline diamond (NCD) cantilevers are expected to provide high quality factor. These structures can be used in many applications including radio-frequency (RF) switch, high speed actuator and sensors<sup>27</sup>.

In this study, a NCD/AlN cantilevers were fabricated and characterized. Actuation has been performed using AlN piezoelectric thin films. These devices are processed using standard MEMS micro-fabrication techniques<sup>28</sup>. Figure 3a shows a SEM picture of NCD/Cr/AlN/Cr cantilever resonator characterized in vacuum conditions using impedance measurement. As shown in figure 3b, piezoelectric actuation has been successfully achieved. The quality factor varies between 1000 to 3000 versus the cantilever length and the resonant mode number.

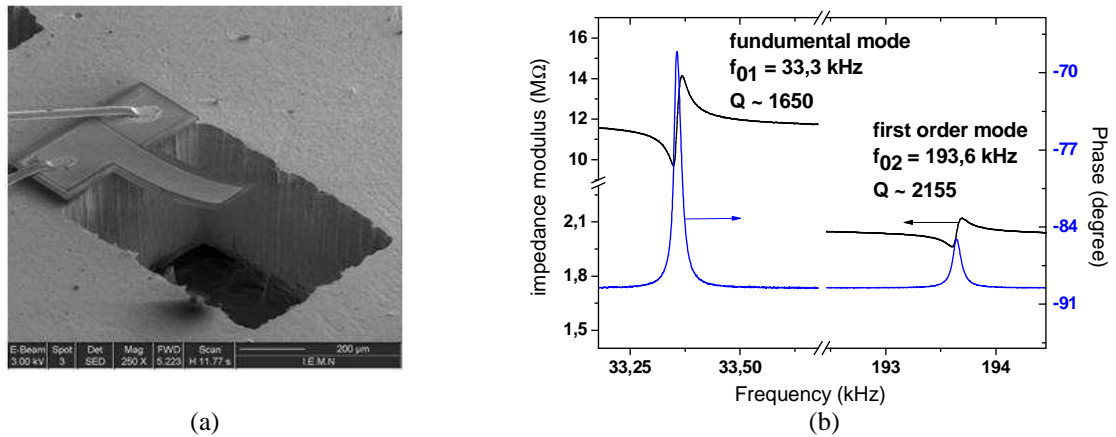


FIGURE 3. (a) SEM picture of NCD/AlN cantilever, (b) Impedance spectra of a 320 μm long and 70 μm wide AlN/NCD cantilever at the first and second resonant modes.

## 4-CONCLUSIONS

In this paper, we have briefly described in the first part the growth techniques of cBN and diamond thin films. In the second part, we have presented three different applications based on the exceptional properties of these wide band gap materials: UV detectors for solar observation, high frequency mechanical resonators and a microcantilever. These photodetectors present extremely low dark current, high breakdown voltage, high responsivity and stability under X-UV irradiation. We have shown that FPAR mechanical resonator, presenting a high electromechanical coupling coefficient, can be design for high frequency filtering. Diamond/AlN microcantilevers present high quality factor in vacuum. These types of devices are expected to be excellent platform for sensor applications.

## REFERENCES

1. W. Torbicz, D. Sobczynska, A. Olszyna, G. Fortunato, A. D'Amico, *Phys. Status Solidi A* **86** (1984) 453.
2. O. Mishima, K. Era, J. Tanaka, S. Yamaoka, *Appl. Phys. Lett.*, **53** (1988) 962.
3. R.H. Wentorf, *J. Chem. Phys. (USA)*, **36** (1962) 1990-1991.
4. Mirkarimi, *J. Mater. Res.*, **9** (1994) 2925-2938.
5. T. Klotzbücher, E. W. Kreutz, *Diam. & Rel. Mat.*, **7** 1219 (1998)
6. Y. Yamada-Takamura, O. Tsuda, H. Ichinose, T. Yoshida, *Phys. Rev. B*, **59** (15) (1999) 10351.
7. W. Kulisch, S. Reinke et R. Freudenstein, *ISAM Tsukuba*, Japan, March 1-5, 1998.
8. W. Otano-Rivera, L.J. Pilione and R. Messier, *Appl. Phys. Lett.*, **72** (20) (1998) 2523.
9. H.B. Luthje, K. Bewilogua, S. Daaud, M. Johansson, L. Hulman, *Thin Solid Films* **247** (1995) 40.
10. X.W.Zhang, H.-G.Boyen, P.Ziemann, M.Ozawa, F.Banhart, M.Schreck, *Dia. and Rel. Mat.*, **13** (2004) 1144-1148.
11. K. Sugawa, M. Ishihara, J. Kim, M. Hasegawa, Y. Koga, *New diamond and frontier carbon technology* **16** (2006) 337.
12. M. Ihara, et al. *Appl. Phys. Lett.*, **65** (1994) 1192.
13. O. A. Williams, O. Douheret, M. Daenen, K. Haenen, E. Osawa, M. Takahashi, *Chem. Phys. Lett.*, **445** (2007) 255.
14. S. Koizumi, C. Nebel and M. Nesladek, Ed. 2008 Wiley-VCH Verlag GmbH & Co. KGaA, Weinheim (2008) 74.
15. S. Koizumi, C. Nebel, M. Nesladek, "Physics and Applications of CVD Diamond" Wiley-VCH Ed. (2008) 85.
16. J. Pernot, P. N. Volpe, F. Omnès, P. Muret, V. Mortet, K. Haenen, T. Teraji, *Phys. Rev., B* **81** (2010) 205203
17. J. Pernot, S. Koizumi, *Appl. Phys. Lett.*, **93** (2008) 052105.
18. V. Mortet, K. Haenen, J. Potmesil, M. Vanecek, M. D'Olieslaeger, *Phy. Stat. Sol. A* **203** (2006) 3185-3190.
19. V. Mortet et al., *Appl. Phys. Lett.*, **81** (2002) 1720.
20. U. Schühle et al., *Proc SPIE* 5171 (2004) 231-238.
21. A. BenMoussa et al., *Nuclear Instruments and Methods A* **568** (2006) 398-405.
22. A. BenMoussa et al., *Dia. and Rel. Mat.*, **18** (2009) 860-864.
23. A. Soltani et al., *Appl. Phys. Lett.*, **92** (2008) 053501.
24. M. Benetti et al., *Ultrasonics, Ferroelectrics and Frequency Control, IEEE Transactions on* **52**(10) (2005) 1806-1811.
25. Z. Chengjie et al., *Ultrasonics, Ferroelectrics and Frequency Control, IEEE Transactions on*, **57**(1) (2010) 82-87.
26. V. Yantchev et al., *Ultrasonics, Ferroelectrics and Frequency Control, IEEE Transactions* **56**(12) (2009) 2701-2710.
27. J. Kusterer, A. Lüker, P. Herfurth, Y. Men, W. Ebert, P. Kirby, M. O'Keefe, E. Kohn, *Dia. and Rel. Mat.*, **17**(7-10) (2008) 1429-1433.
28. V. Mortet, A. Soltani, A. Talbi, P. Pobedinskas, K. Haenen, J-C. De Jaeger, P. Pernod, P. Wagner, *Procedia Chemistry*, **1**(1) (2009) 40-43.